Proceedings of the 11th World Congress on New Technologies (NewTech'25)
Paris, France - August, 2025
Paper No. ICNFA 119
DOI: 10.11159/icnfa25.119

Evaporation and Fluid Dynamics of a Multicomponent Sessile Droplet on Nanostructured Doubly Reentrant Surfaces

Xin Ye[1], Huihe Qiu[1,2]
[1]Sustainable Energy and Environment Thrust,
The Hong Kong University of Science and Technology (Guangzhou),
Nansha, Guangzhou, China 511453
meqiu@hkust-gz.edu.cn
[2]Department of Mechanical and Aerospace Engineering,
The Hong Kong University of Science and Technology,
Clear Water Bay, Kowloon, Hong Kong SAR, China
meqiu@ust.hk

Abstract – The fluid dynamics and evaporation of a sessile multicomponent droplet on nanostructured doubly reentrant surfaces are complex and du to superhydrophobic wettability of the surfaces. This kind surface is very promising in controlling droplet dynamics, heat transfer and evaporation. In this paper, we investigate the interfacial effects of nanostructured doubly reentrant surfaces on the flow behaviors and local concentration evolution during the evaporation of an ethanol/water multicomponent droplet. Using micro-resolution particle image velocimetry (μPIV) and novel aggregate-induced emission-based (AIE) techniques, the flow patterns and local concentration distributions on both hydrophobic and nanostructured doubly reentrant surfaces are probed and compared. It is found that in addition to the established Marangoni flow dominated stage, transition stage, and buoyancy-induced flow dominated stage, a new transition stage and rolling stage for the nanostructured doubly reentrant surface are detected in the late evaporation period. Differences in the local concentration distribution evolution occur, depending on the hydrophobicity of the surface on which the droplet is placed. The theoretical analysis combining PIV and AIE visualization results reveals that the variations in droplet concentration distributions on surfaces with different hydrophobicity exert a significant impact on evaporative behaviors. These behaviors in turn affect the evolution of local concentration distribution.

***Keywords*:** Nanostructure, Doubly Reentrant Surface, Micro Fluid Flow, Superhydrophobic, Evaporation, Multicomponent

1. Introduction

The evaporation of a sessile droplet on a solid surface is crucial phenomenon in nature, and it is critical for various applications including inkjet printing, micro- and nano-fluidics, thermal management, combustion engineering, DNA self-assembly, etc. Previous research mainly focused on monocomponent droplets, but droplets in industrial applications usually contain two or more miscible components rather than a single component. Also, they do not consider the surface wettability effect on the fluid dynamics and evaporation processes. Previous studies focused on parameters affecting the evaporation rate, evaporation behaviors and flow regimes inside a multicomponent droplet. Katre et al.20 reported the concentration distribution inside multicomponent droplets inferred from the infrared (IR) images, but no exact concentration value was provided. Siddiqui *et al*. investigated the phase change dynamics of the CAHF droplet over heated plain copper and porous residue (formed by the evaporation of the first CAHF droplet on a plain copper surface) surfaces. They demonstrated that the evaporation rate for CAHF droplets resting on their partially wetting residue surfaces substantially improved compared to that on a non-wetted plain copper surface in sub-boiling and nucleate boiling regimes [1]. He *et al*. systematically investigated the evaporation dynamics of the droplet during the evaporation process on hydrophobic network surfaces, containing the constant pattern fraction (f p = 0.1) and various pattern sizes [2]. Analyzing the time evolution of the contact angle and the contact base diameter, four major evaporation stages (i.e., CCL, CCA, PP, and MCL) and different time durations were distinguished, which was largely dependent on the substrate patterns (i.e., surface patterns' scale and structure). Siddiqui *et al*. studied the evaporation and boiling behaviors for various mixing ratios of the silver-graphene hybrid nanofluid (SGHF) droplet on heated copper and their own residue surfaces. We investigated the effects of the synergistic

thermal conductivity and the thermal Marangoni convection on evaporation performance of the SGHF droplet over heated surfaces. Based on our experimental and numerical findings, we developed a diffusion-convection evaporation model that can predict the SGHF droplet evaporation rate on heated surfaces in a temperature range of 25 °C ≤T s ≤100 °C. Our results showed that the SGHF droplet evaporation and boiling performance highly depend on its mixing ratio [3]. With the development of aggregation-induced emission (AIE) luminogens, local concentration measuring becomes possible. AIE luminogens dissolved in a high-solubility solvent are almost non-emissive. When a poor solvent is added, AIE luminogens show a dramatic increase in fluorescence emission due to the formation and accumulation of aggregates, which is called AIE effect. Using this characteristic of AIE luminogens, local concentration distribution of a multicomponent droplet can be derived from the intensity of fluorescence emission. Cai *et al.* [4] first applied AIE luminogens in concentration probing of THF/water multicomponent droplets on a hydrophobic surface. The local concentration distribution in sessile multicomponent droplets during a quasi-static evaporation process was visualized. This novel technique provides the potential to measure the local concentration distribution of the ethanol/water multicomponent, which is one of the most common types of multicomponent droplet both in research and industrial areas.

In this study, we report the interfacial effects of nanostructured doubly reentrant surfaces on evolution of local concentration and fluid flow in an evaporating multicomponent droplet. We first conducted PIV to visualize the evaporative flow behaviors inside the ethanol/water multicomponent on a nanostructured doubly reentrant surface. Additionally, the AIE-based local concentration tracking technique is used to measure the local concentration distribution evolution during the evaporation lifetime of the droplet on two types of surfaces with different wettability. To date, the characteristics of doubly reentrant surfaces supporting low surface tension liquids have predominantly been utilized for liquid-repellent and self-cleaning surfaces. However, further research is needed to understand the evaporation processes and mechanism behind such surfaces. The usage of nanostructured doubly reentrant surface provides a method to reduce the evaporation rate, which could be utilized in some biochemical and pharmaceutical industries to inhibit unexpected fast evaporation. Additionally, the changes in evaporation modes could also be used to control the deposition patterns of particles in a droplet. We found the local concentration distribution evolution on the nanostructured doubly reentrant surface is significantly different from that on the hydrophobic surface, especially during the late period of droplet evaporation. In the present work, local concentration changes caused by a rolling flow pattern in a multicomponent droplet on a nanostructured doubly reentrant surface are observed experimentally and analyzed for the first time.

2. Experimental Setup

As shown in Figure 1a, the hydrophobic surface adopted in this work is fabricated on a 2 cm × 2 cm transparent glass surface with a 100 nm-thick ITO layer which serves as a resistive heater (Kintec Company). Two 300 nm-thick gold layers are fabricated on the ITO surface as the electrodes. The water contact angle of the hydrophobic surface is 106° (± 2°), as shown in Figure 1b. Following the process flow illustrated in Figure 1c, the nanostructured doubly reentrant surface (Figure 1d) is fabricated. A 1-μm-thick silica layer was fabricated by wet oxidation, which was partially etched in subsequent steps, resulting in a final overhanging edge with a thickness of ~500 nm. More detailed fabrication processes can be found in our previous research30. Owing to the special structure, this surface can suspend low-surface-energy liquid like ethanol to a Cassie state, giving a higher contact angle as 154° (± 1°) of 96% ethanol, as shown in Figure 1e. Fabrication details can be found in Ref.30 and the scanning electron microscopy (SEM) image of the finished product is shown in Figure 1f.

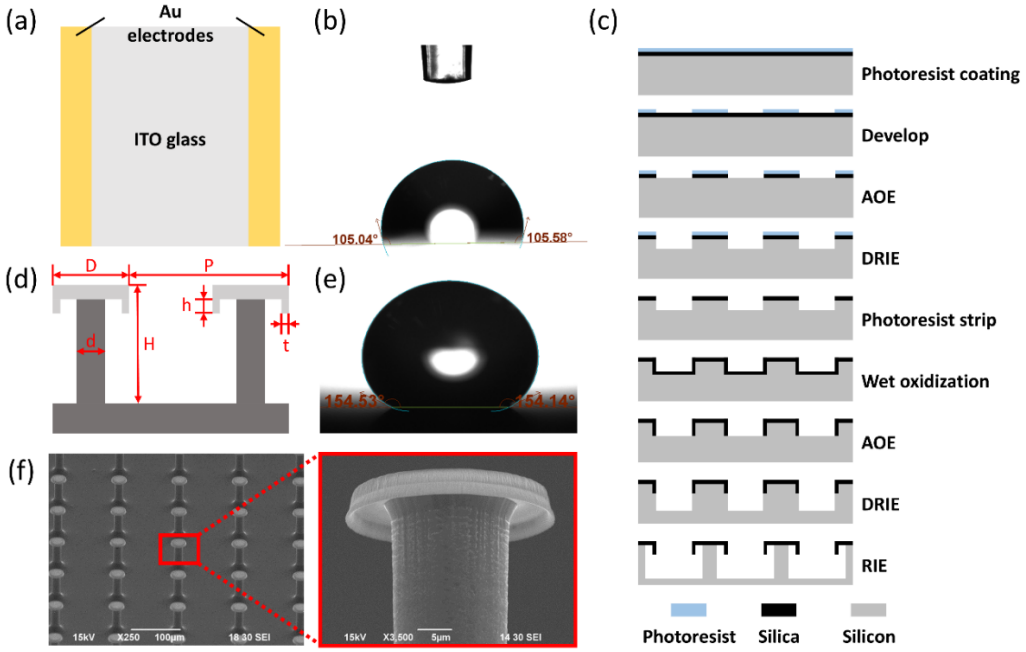

Figure 1. (a) Schematic of the hydrophobic surface. (b) Static contact angle of pure water on the hydrophobic surface. (c) Fabrication process flow of the nanostructured doubly reentrant surface. (d) Schematic of the doubly reentrant structure on the nanostructured doubly reentrant surface (P = 120 μm, D = 30 μm, d= 15 μm, H = 55 μm, h = 2.5 μm, t = ~500 nm). (e) Static contact angle of 96% ethanol on the nanostructured doubly reentrant surface. (f) SEM images of the nanostructured doubly reentrant surface.

The multicomponent droplet was generated from a mixture of deionized water and ethanol, with an initial water fraction of 60% vol. In the evaporative flow measurements by PIV, the multicomponent solution was seeded with dyed aqueous fluorescent particles (Fluoro-Max R0300, Thermo Scientific), which have an emission peak of 612 nm. The concentration of the seeding particles is 0.05% vol.

AIE luminogens were adopted to measure the local concentration inside the multicomponent droplet. An AIE luminogen (AIETM pH, AIEgen Biotech Co., Limited) proved to be soluble in ethanol, and its solubility is poor in water31. Based on the AIE effect mentioned before, the fluorescence intensity of this AIE luminogen exhibits an increasing tendency as water fraction increases. This AIE luminogen, which is sensitive to concentration was used to track the local concentration during the evaporation process of ethanol/water multicomponent droplets. The excitation peak and emission peak of this AIE luminogen were ~440 nm and ~625 nm, respectively. Saturated AIE luminogen solution was prepared by adding ethanol to AIE luminogens until complete dissolution, as a stock solution. 2 μL stock solution was transferred to an EP-tube, and then an appropriate amount of ethanol and deionized water was added to obtain 15 μL multicomponent mixture with 60% vol. water fraction. The aggregates of AIE luminogens have high thermal stability under 298 ℃, while the surface temperature is 48 ℃ in our experiments. Thus, these AIE luminogens are stable during the entire experiment process.

The schematic of the experimental setup is shown in Figure 2. A 6 ± 0.1 μL multicomponent droplet was generated by a 10 μL syringe (700 Series Hand-fitted Syringe, Hamilton), and then gently and vertically placed on the surface. To achieve equivalent heating conditions in both cases, the surface temperature was maintained at a constant 48 ± 0.1 ℃ by accurately adjusting the power of DC power supply. The ambient temperature was controlled at 25 ± 2 ℃. A laser system with a wavelength of 450 nm was used as the excitation source for fluorescent tracer particles in PIV experiments and AIE luminogens in concentration tracking experiments. For the transparent hydrophobic surface, a laser was generated and expanded to a light sheet to illuminate the central profile of the droplet from the bottom, and the ITO layer powered by a DC power supply heated the surface directly. As the nanostructured doubly reentrant surface was opaque, the laser sheet

illuminated the central profile from the side. A ceramic heater below the surface, which was also powered by the DC power supply, was used to heat the surface. The measured value of the laser power density P at the droplet location was 37.9 ± 0.1 mW/mm^2. A high-speed CCD camera (FASTCAM SA-Z, Photron) with a macro lens (MP-E 65mm f/2.8 1-5x Macro Photo, Canon) was utilized to record images under a resolution of 1024 × 1024 pixels during droplet evaporation. The magnification of the lens was adjusted to 2.2 × to achieve a balance between the light inlet and the field of vision.

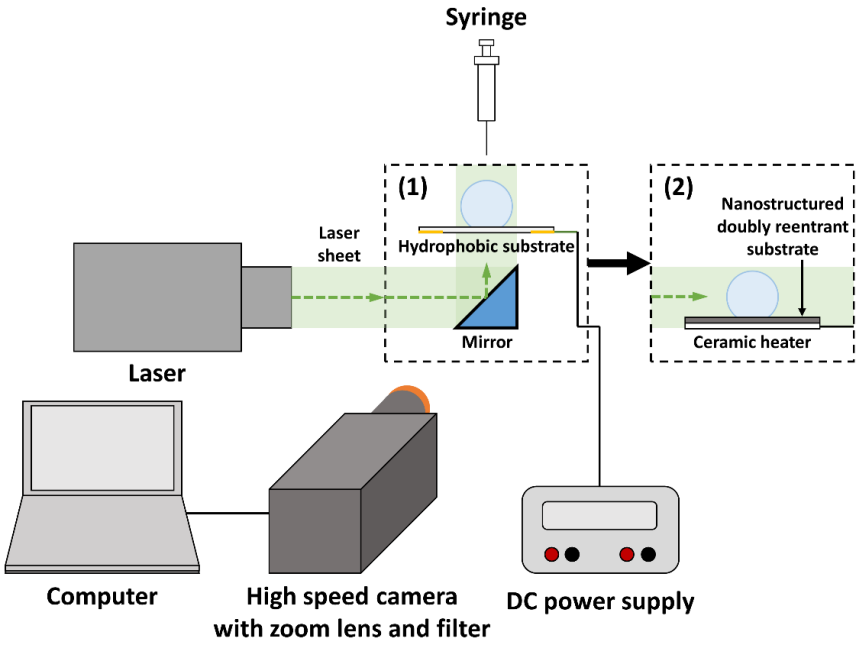

Figure 2. Schematic of the experimental setup: (1) for hydrophobic surface; (2) setup for nanostructured doubly reentrant surface.

Table 1. Parameters of the experimental setup for PIV experiments and AIE-based concentration tracking experiments.

	Droplet volume (μL)	Wavelength of laser (nm)	Filter	Surface temperature (°C)	Frame rate (fps)	Shutter time (s)
PIV experiments	6	450	550 nm long-pass filter	48	125	1/2000
AIE-based concentration tracking experiments	6	450	550 nm long-pass filter	48	125	1/1000

Velocities of particles were obtained by PIV. A multi-pass, cross-correlation algorithm for velocity calculation was used. Assuming that the droplet has a spherical cap shape, a velocity correction algorithm reported by Kang *et al.* [5] and revised by Minor *et al.* [6] was applied to eliminate the effect of refraction.

3. Results and Discussion

Figure 3 illustrates the internal flow behaviors inside the multicomponent droplet on the nanostructured doubly reentrant surface. The evaporation process can be divided into five stages based on the characteristics of flow behaviors. The first three stages include a Marangoni flow dominated stage, a transition stage, and a buoyancy-induced flow dominated stage, which are similar to those of a multicomponent droplet on the hydrophobic surface, as shown in Figure 3a-c. The Marangoni effect weakens and even disappears as ethanol is consumed; thus the buoyancy-induced flow is increasingly dominant. Hence, the flow direction at the central axis gradually transfers from downward to upward. In the fourth stage (see Figure 3d), the two vortices become asymmetric with one vortex becoming larger and the other becoming smaller, which is another transition stage. This is because the rolling flow is comparable with the buoyancy-induced flow, resulting in a temporary unsteady flow pattern. A gradual transition from two symmetric vortices to an asymmetric single roll vortex takes place with the increasing strength of rolling flow. Then, it transfers to the fifth stage after full development of the transition flow pattern with a distinct rolling flow pattern inside the multicomponent droplet, as shown in Figure 3e. This rolling flow pattern can be observed only when the length scale of the droplet is smaller than a critical value. By evaluating the average vorticity, we can divide the symmetric flow pattern and asymmetric flow pattern. Vorticities exhibit a smaller averaged absolute value (0.32 s-1 in the buoyancy-induced flow dominated stage) with higher variance in the symmetric flow pattern. In contrast, the asymmetric flow pattern demonstrates a larger averaged absolute vorticity (4.76 s-1 in the rolling stage) and lower variance of vorticities. Under the high laser power used in this work, the influence of photobleaching effect on fluorescence intensity is non-negligible. Photobleaching is a photo-chemical reaction that will irreversibly destroy the fluorophore molecules due to the excitation[7]. Thus, fluorophore molecules will lose their capability to fluoresce, resulting in a decline in the total fluorescence intensity as time exposed to the laser increases. To accurately track local concentration evolution, nondimensional intensity versus time exposed to the laser under experimental laser power (37.9 mW/mm^2) is measured and plotted, where the nondimensional intensity is obtained by dividing the intensity by the initial intensity (exposure time = 0 s). Under current experimental conditions, the effect of temperature on calibration is negligible since luminous intensity of AIE is not temperature sensitive. Three measurements are conducted for every water fraction. When the fraction of water, a poor solvent for the AIE luminogen, progressively rises, the fluorescence intensity gradually increases. Notably, the fluorescence intensity significantly increases within the range from 65% vol. to 75% vol. The fluorescence intensity at a water fraction of 85% vol. is ~12-fold that in the solution with a water fraction of 50% vol.

Unlike the consistent concentration distribution in a multicomponent droplet on the hydrophobic surface, continuously changing local concentration distribution on the nanostructured doubly reentrant surface is observed, as shown in Figure 4. In the early evaporation stage, uniform concentration distribution is observed, as shown in Figure 4a and b. The reason can be explained as follows. The dominant flow behaviors in the early evaporation stage are downward Marangoni flow (see Figure 3a) and transition flow (see Figure 3b) sequentially, with furious and chaotic vortices near the liquid-air interface. Thus, ethanol and water migrate around the droplet, contributing to the uniform concentration distribution. According to results of the flow field measurement, this early stage lasts until approximately 28 s, which is consistent with the experimentally measured local concentration change.

Then, a strip-shaped high-water-fraction region is gradually formed at the center of the droplet during the first transition stage (see Figure 4c and d) and finally established in the intermediate evaporation stage (see Figure 4e). This phenomenon is attributed to the flow behaviors in the buoyancy-induced flow dominated stage (see Figure 3c) as discussed above (before ~92 s). Water fraction increases initially in the surface region due to the preferential evaporation of ethanol. Besides, for the droplet with a contact angle larger than 90°, the evaporation rate at the upper part of the droplet is much higher than that at the lower part. Therefore, Marangoni flow caused by the largest concentration difference occurring between the upper region and the lower inner region, which synergizes with the buoyancy-induced flow, leads to a component migration upwards from the lower region to the apex. As a result, the transport route of water is downward along the surface, inward radially to the center, and upward along the central axis in this stage. Therefore, massive water is transported to the center of the multicomponent droplet to form a strip-shaped high-water-fraction region at the central axis, as shown in Figure 4e. Moreover, the flow pattern in this stage is symmetric, leading to an axial symmetric concentration distribution. According to the symmetry, the concentration gradient at the central axis in the horizontal direction equals to 0. Hence, water in the middle part is not transported sideways by the concentration-gradient-induced solutal Marangoni flow. Besides, water at the

central axis moves upward rather than laterally because the direction of buoyancy is upward. Because the diffusion process is slow, the stripe-shaped high-water fraction region can exist steadily during the buoyancy-induced flow dominated stage until the flow pattern begins the transition to the rolling flow pattern.

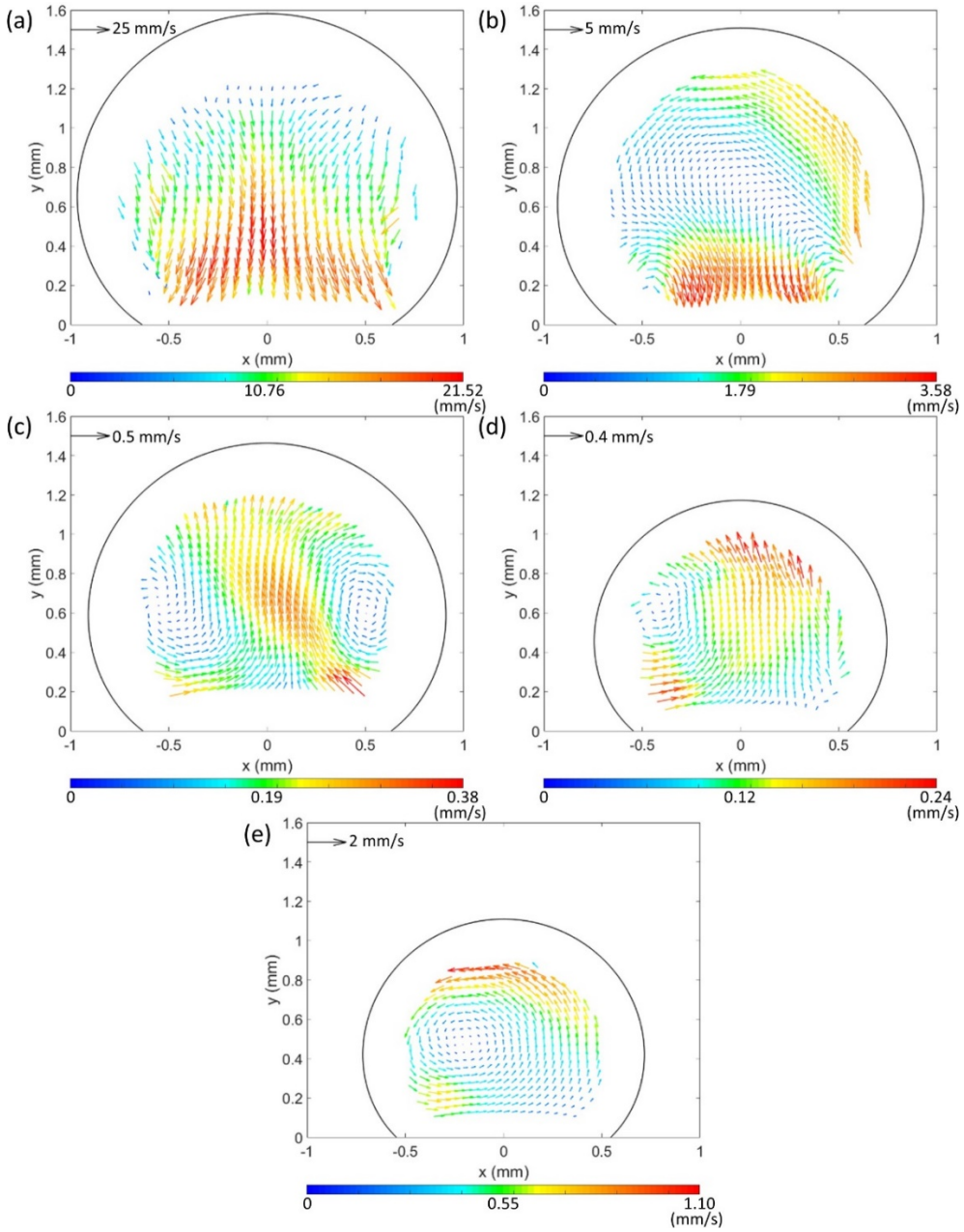

Figure 3. Evaporative internal flow patterns of an ethanol/water multicomponent droplet on a nanostructured doubly reentrant surface measured by PIV (initial water fraction: 60% vol., surface temperature: 48 °C) in five stages: (a) Marangoni flow dominated stage (downward at central axis); (b) first transition stage; (c) buoyancy-induced flow dominated stage (upward at central axis); (d) second transition stage; and (e) rolling stage.

The concentration distribution changes again in the second transition stage (see Figure 4f and g) and the late stage (see Figure 4h), affected by the generation of the rolling flow pattern (see Figure 3e). This stage begins at around 129 s, which coincides with the rolling stage (Figure 3e). Due to the change of the geometrical parameters (mainly the length scale L) of the droplet, the balance of the steady symmetric buoyancy-induced flow field is broken and the flow field transforms to the rolling flow field. Two components are re-distributed throughout the entire droplet under the effect of the rolling flow. Thus, the stripe-shaped region with high water fraction is destroyed and the concentration distribution changes, as shown in Figure 4f and g. After the unstable transition stage, a steady shell-shaped high-water fraction region is observed near the liquid-air surface owing to the evaporation of ethanol from the surface, as shown in Figure 4h. The concentration distribution corresponds to the distribution of evaporative flux. For the droplet with a contact angle larger than 90°, evaporative flux shows the highest value at the apex and decreases downward gradually along the liquid-air surface, finally reaching a minimum value at the triple line. Hence, in our experiments, at the apex region of the droplet where evaporative flux is maximum, the local water fraction is the largest, and the local water fraction decreases along the liquid-air interface with the reducing evaporative flux. The local water fraction at the triple line region is lower than that at the apex region due to the low evaporative flux. Besides, because the flow velocity in this rolling stage is high enough, ethanol consumed by evaporation can be replenished by the rolling flow promptly. Consequently, this concentration distribution can be maintained during the whole late stage.

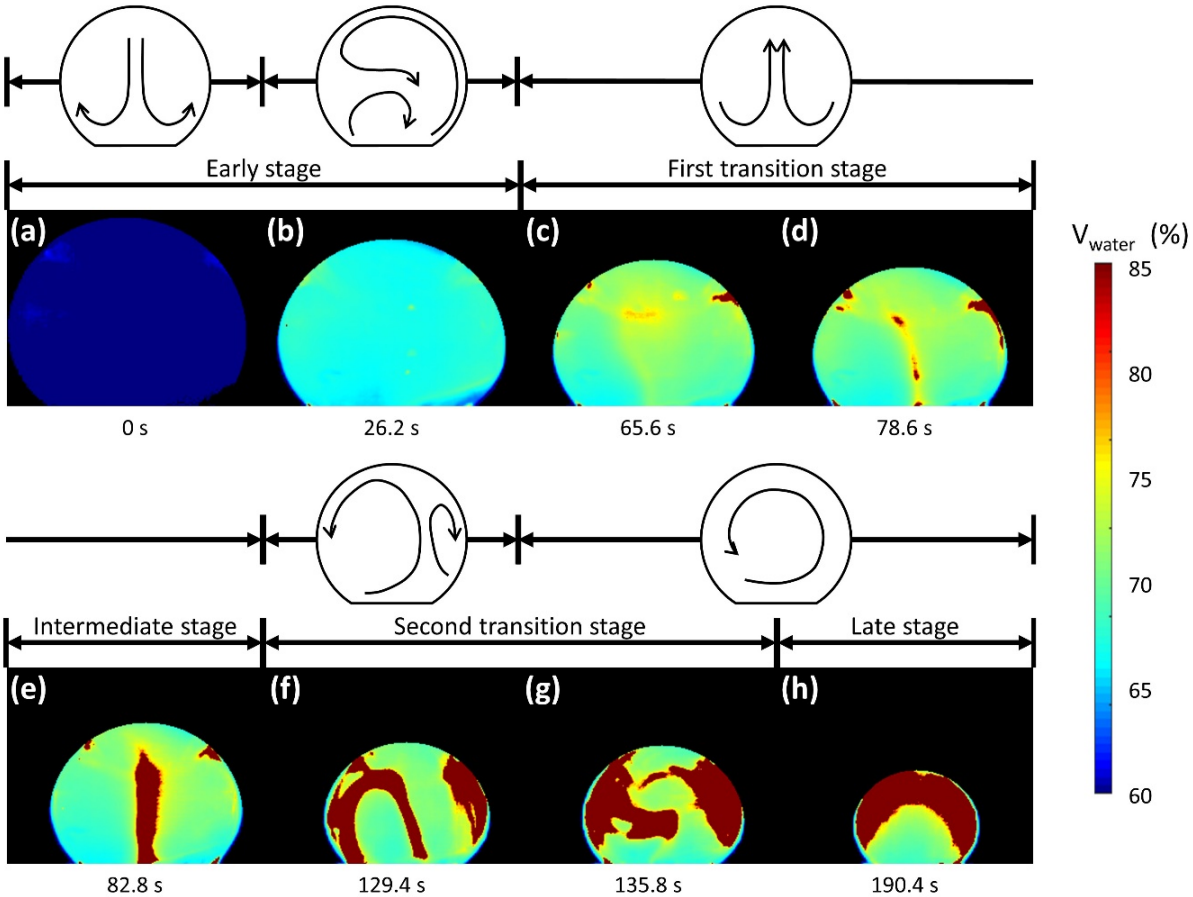

Figure 4. Concentration profiles and corresponding flow behaviors of a multicomponent droplet on the 48 °C nanostructured doubly reentrant surface with an initial water fraction of 60% vol.: (a) initial status; (b)-(h) concentration evolution in time sequence.

4. Conclusion

Our work indicates that interfacial wettability and structure of a surface plays a crucial role in affecting both the local concentration and internal fluid flow dynamics. In this work, the interfacial effects of nanostructured doubly reentrant surfaces on evolution of local concentration and fluid flow in an evaporating multicomponent droplet were experimentally studied and compared with that on a hydrophobic surface via AIE-based local concentration tracking technique and PIV.

Unlike three stages of internal flow behaviors were observed on the hydrophobic surface, five stages were found on the nanostructured doubly reentrant surface. A rolling stage followed by a transition stage occurs when superhydrophobicity is large enough to support a multicomponent droplet with a high aspect ratio. Local concentration distribution evolution on the nanostructured doubly reentrant surface is also significantly different from that on the hydrophobic surface, especially during the late evaporation period. For the multicomponent droplet on the nanostructured doubly reentrant surface, local concentration distribution changed over time. The concentration distribution in the multicomponent droplet exerts a phased influence on the internal flow field, while the internal flow reciprocally affects the concentration distribution in a coupled manner. Local concentration changes caused by a rolling flow pattern in a multicomponent droplet on a nanostructured doubly reentrant surface are first observed experimentally and analysed in this work.

Acknowledgements

This research is supported by Guangdong Basic and Applied Basic Research Foundation (2021B1515130008) and Science and Technology Planning Project of Guangdong Province (2023A0505030005). The authors acknowledge assistance from the Nanosystem Fabrication Facility (NFF) of HKUST for the device/system fabrication.

References

[1] F.R. Siddiqui, C.Y. Tso, H.H. Qiu, Christopher Y. H. Chao, S.C. Fu (2022) Copper-alumina hybrid nanofluid droplet phase change dynamics over heated plain copper and porous residue surface, International Journal of Thermal Science, 182 (2022) 107795.

[2] Minghao He, Yinchuang Yang, Mei Mei and Huihe Qiu. (2022): "Droplet Evaporation Dynamics on Hydrophobic-Network Surfaces," Langmuir, 2022, 38, 20, 6395–6403, https://doi.org/10.1021/acs.langmuir.2c00479.

[3] F.R. Siddiqui, C.Y. Tso, S.C. Fu, H.H. Qiu, Christopher Y. H. Chao (2021): "Droplet evaporation and boiling for different mixing ratios of the silver-graphene hybrid nanofluid over heated surfaces," International Journal of Heat and Mass Transfer, Volume 180, December 2021, 121786.

[4] Cai X, Xie N, Qiu ZJ, Yang JX, He MH, Wong KS, Tang BZ and Qiu H.-H. (2017): "AIEgen based direct visualization of concentration gradient inside an evaporating binary sessile droplet, *ACS Applied Materials & Interfaces*, v. 9, (34), Aug 2017, p. 29157-29166.

[5] Kang, K. H.; Lee, S. J.; Lee, C. M.; Kang, I. S. Quantitative Visualization of Flow inside an Evaporating Droplet Using the Ray Tracing Method. Meas. Sci. Technol. 2004, 15, 1104.

[6] Minor, G.; Oshkai, P.; Djilali, N. Optical Distortion Correction for Liquid Droplet Visualization Using the Ray Tracing Method: Further Considerations. Meas. Sci. Technol. 2007, 18, L23-L28.

[7] Vicente, N. B.; Zamboni, J. D.; Adur, J. F.; Paravani, E. V.; Casco, V. H. Photobleaching Correction in Fluorescence Microscopy Images. In J. Phys. Conf. Ser. 2007; Vol. 90, pp 1-8.